AJRCCM Articles in Press. Published on 19-October-2018 as 10.1164/rccm.201802-0352OC

Title: Increased IgA expression in lung lymphoid follicles in severe COPD

Maha Zohra Ladjemi[1,3], Clémence Martin[7], Marylène Lecocq[1,2], Bruno Detry[1,3], Frank Aboubakar Nana[1], Charlotte Moulin[1], Birgit Weynand[5], Chantal Fregimilicka[6], Caroline Bouzin[6], Pascal Thurion[4], François Carlier[1], Jef Serré[9], Ghislaine Gayan-Ramirez[9], Monique Delos[4], Sebahat Ocak[1,8], Pierre Régis Burgel[7] and Charles Pilette[1,2,3]

Authors's affiliations: [1]Université Catholique de Louvain (UCL), Institut de Recherche Expérimentale & Clinique (IREC), Pôle de Pneumologie, ORL & Dermatologie Brussels, Belgium ; [2]Cliniques universitaires St-Luc, Service de Pneumologie Brussels, Belgium ; [3]Institute for Walloon Excellence in Lifesciences and Biotechnology (WELBIO), Brussels, Belgium ; [4]CHU de Mont-Godinne, Service d'anatomopathologie; Yvoir, Belgium ; [5]UZ Leuven, Pathologische Ontleedkunde, Leuven, [6]Université Catholique de Louvain (UCL), Institut de Recherche Expérimentale & Clinique (IREC), IREC Imaging Platform Brussels, Belgium ; [7]Université Paris Descartes, Sorbonne Paris Cité, 75005 Paris, France ; Service de pneumologie, hôpital Cochin, AP-HP, 27, rue du Faubourg-Saint-Jacques, 75014 Paris, France ; [8]CHU UCL Namur (Site Godinne), Service de Pneumologie; Yvoir, Belgium. [9]KULeuven, Laboratory of respiratory diseases; Leuven, Belgium.

Corresponding author: Pr Charles Pilette, e-mail: charles.pilette@uclouvain.be; Phone: +32 2764 5486; Fax: +32 2764 9440.

Author's contribution: MZL carried out most of experiments, most of data analysis, co-supervised the experimental design and wrote the manuscript, CM carried out mice experiments, ML carried out RT-qPCR experiments, CM performed in vitro experiments on B cells, BW analyzed with MZL the IHC stainings as a second pathologist and

Copyright © 2018 by the American Thoracic Society

provided lung tissue samples, FA and SO helped for IHC stainings and analyses, PT made a part of IHC stainings, JS and GGR performed the model of smoking mice, MD provided lung tissue samples, CF made the tissue processing and a part of IHC stainings, CB helped for IHC data analysis, FC made and analyzed the IL-21/ B and T cells co-localization by IF staining, BD helped for quantification of IHC stainings and advice, PRB supervised the design of the in vivo study, CP supervised the design of the study, patient recruitment, data analysis, and writing of the manuscript.

Grants: CP is postdoctoral specialist of the Fonds National de la Recherche Scientifique, Belgium (Grant FRSM 3.4522.12 and mandate #1.R.016.14) and was investigator of the Institute for Walloon Excellence in Lifesciences and Biotechnology (WELBIO CR-2012S-05). MZL and BD were supported by the Institute for Walloon Excellence in Lifesciences and Biotechnology (WELBIO CR-2012S-05).

Running title: Lung follicular IgA in COPD

Total word count: 3290

At a Glance Commentary: Scientific Knowledge on the Subject. Chronic obstructive pulmonary disease (COPD) is associated with aberrant immune and structural responses of the airways to inhaled toxics. While accumulation of B cells and lymphoid follicles has been described in COPD airways, the functional status of lung B cells remains poorly known. **What This Study Adds to the Field.** This study demonstrates upregulated IgA expression in lung lymphoid follicles from severe COPD patients, suggesting exacerbated IgA immune response against foreign (e.g., microbial) and/or self-antigens in severe disease. **Online Data Supplement:** This article has an online data supplement, which is accessible from this issue's table of content online at www.atsjournals.org

Copyright © 2018 by the American Thoracic Society

AJRCCM Articles in Press. Published on 19-October-2018 as 10.1164/rccm.201802-0352OC

Abstract

Rationale: Accumulation of B cells and lymphoid follicles (LF) has been described in chronic obstructive pulmonary disease (COPD) airways, but the functional status of lung B cells remains poorly known. **Objectives:** The aim of this study was to characterize LF for expression of IgA, the main mucosal antibody. **Methods:** The presence of B cells and LF, including intra-follicular IgA expression, were determined in the lung from COPD patients (n=37) versus controls (n=34) by immunohistochemistry. We also evaluated follicular IgA responses in the lungs from mice infected with *Pseudomonas aeruginosa* (PAO1) (n=10 per group) and in smoking mice. **Measurements and main results:** Whereas in smokers B cell numbers slightly increased, robust increases in B cell and LF numbers (mainly in distal airways) were only observed in severe COPD. The majority of follicular B cells were IgM+ (70-80%), but IgA+ (and not IgG+) B-cell numbers were increased in LF from severe COPD compared to controls (two-fold, 44.7% vs 25.2%), and this was significant in distal but not proximal airways. Follicular IgA response was also observed in PAO1-infected mouse lungs, but not following smoke exposure. Moreover, follicular IgA expression associated with expression of IL-21, which was very potent to activate Ig production in vitro. **Conclusions:** This study shows that IgA production occurs in peribronchiolar LF from severe COPD, where IL-21-producing T cells are present, and presumably represents a feature of exacerbated mucosal adaptive immune responses against microbial and/or self-antigens.

Abstract word count: 236

Key words: COPD, lymphoid follicles, B Lymphocytes, IgA

Copyright © 2018 by the American Thoracic Society

Introduction

Chronic obstructive pulmonary disease (COPD) is a lung disorder associated with aberrant immune and structural responses of the airways to inhaled toxics, including accumulation of neutrophils, macrophages and CD8+ T-cells (1, 2). Accumulation of B cells has been reported more recently in COPD, with organization into so-called tertiary lymphoid follicles (LF) (3) in both proximal (4) and distal airways particularly from patients with severe disease and emphysema (5). LF consist of specific arrangements of B cells, T cells and follicular DCs which allow priming and clonal expansion of T and B cells. Several mediators support lymphoid neogenesis in the COPD lung (6-8), including CXCL13 (9, 10), BAFF (11, 12), IL-17(13) as well as CXCR3 ligands (14).

Immunoglobulin A (IgA) is a major first-line mechanism of defense at mucosal surfaces, including the airways. It is produced as dimeric IgA (dIgA), which is able (unlike monomeric IgA) to bind to the epithelial polymeric immunoglobulin receptor (pIgR) that mediates its transcytosis into mucosal secretions. We and others have shown that the COPD lung is characterized by a subepithelial accumulation of IgA and related immune complexes (15-17) which is due to increased production (15) and reduced pIgR-mediated transepithelial transport (18). Increased IgA production in the COPD lung is associated with increased levels of BAFF and APRIL (11, 12, 15), which represent cytokines able to induce class-switch recombination to IgA (19). It remains however unclear whether follicular B cells are switched in COPD to IgA production, as the functional status of these B cells remains so far elusive. In addition, the regulation of IgA production in follicular B cells is likely to differ from that in extrafollicular B cells (reviewed in (20)).

Copyright © 2018 by the American Thoracic Society

AJRCCM Articles in Press. Published on 19-October-2018 as 10.1164/rccm.201802-0352OC

The aim of this study was therefore to characterize follicular B cells in the airways from COPD patients for IgA expression, as well as the role of IL-21, which is poorly understood in this setting. Follicular IgA responses were also assessed in the lungs from mice chronically infected with *Pseudomonas aeruginosa* (PAO1) beads (21) as an *in vivo* model of lung LF formation, and from mice exposed to cigarette smoke.

Copyright © 2018 by the American Thoracic Society

Methods

Patients and lung tissue samples. Seventy-one patients, including 34 control patients (i.e. with normal lung function, among whom 21 never smokers, 6 ex-smokers and 7 current smokers); and 37 COPD patients undergoing lung surgery, either for resection of a solitary tumor (n=20) or for transplantation for very severe (GOLD IV) COPD (n=17) were included in the study (Table 1). A smoker was requested to have quitted smoking at least for 6 months before surgery to qualify as former/ex-smoker. No patient received preoperative chemo- or radiotherapy, and patients did not have respiratory exacerbation or infection within the last 6 weeks before surgery. Groups were well matched for gender, age and smoking histories, except a slight significant difference in age between non-smokers and GOLD stage I-II COPD patients (and the fact that almost all severe COPD were ex-smokers). After surgical removal, lung tissue was sampled (largely, at least 5cm, away from the tumor site), to obtain two to five proximal and distal samples for IHC (immediately immersed in 4% formaldehyde) and two samples for RT-qPCR (immediately immersed in RNAlater).

In vivo model of persistent lung infection with Pseudomonas aeruginosa. Mice were infected as previously described (22). Briefly, sterile agarose beads and agarose beads coated with the PA strain PAO1 (median size of the beads, 300 μm) were instilled. Mice were sacrificed at day 14 or 28 and lungs were removed through the right heart for histological analysis and the bronchoalveolar lavage (BAL) was harvested for ELISA analysis.

In vivo model of COPD upon cigarette smoke exposure. Eight weeks old male C57Bl/6JolaH mice were randomly divided into 2 groups: air- or cigarette smoke. At

Copyright © 2018 by the American Thoracic Society

AJRCCM Articles in Press. Published on 19-October-2018 as 10.1164/rccm.201802-0352OC

sacrifice, BAL was performed in mice before heart-left lung block removal, fixation in 6% paraformaldehyde, and embedding in paraffin to assess Ig's in lymphoid aggregates.

Human B cell isolation and stimulation. Blood B cells were separated by magnetic cell sorting using CD19+ microbeads (Miltenyi Biotec), and cultured in the presence or not of LPS (1 μg/ml), cigarette smoke extract (5%), IL-21 (50 ng/ml; kind gift from L. Dumoutier, UCL, Brussels, Belgium), and/or CD40 ligand through irradiated 3T6-CD40L cells (100,000 cells/well; kind gift from Pr. P. Van der Bruggen, UCL, Brussels, Belgium). Cell-free supernatants were harvested at day 6 and day 13 for Ig's detection by ELISA and B cells were harvested for viability or proliferation studies respectively by staining with propidium iodide (PI) or carboxyfluorescein succinimidyl ester (CFSE) as previously described (15).

Immunohistochemistry (IHC). The specimens were incubated overnight at 4°C with *ready-to-use* mouse anti-human CD20 mAb (Clone L26) (Dako, Denmark) or rabbit anti-human CD21 mAb (Clone EP64) (BioSB, USA), respectively revealed with the Ultra View Universal DAB or Alkaline Phosphatase Red detection kits (Roche, Switzerland). The reaction was stopped by washing in water, and slides were counterstained also in the Benchmark XT machine with hematoxylin I or Bluing Reagent. CD20 has been used as pan-B cell marker and CD21 for follicular dendritic cells (FDCs), whereas CD21 may also stain mature B cells in frozen (and not paraffin-embedded) sections.

For Ig staining in human lungs, the following Abs were used respectively for IgM, IgG and IgA staining: biotin-conjugated Abs goat anti-human IgM (B2641, Sigma, USA), rabbit anti-human IgG (Southern Biotech, USA) and unlabeled mouse anti-human IgA mAb (Thermo Scientific, USA) followed by streptavidin-HRP or anti-mouse HRP

Copyright © 2018 by the American Thoracic Society

conjugated Ab. The reaction was developed by incubation with 0.6 mg/ml diaminobenzidine (SigmaFast DAB, Sigma, USA). In murine lungs, rabbit anti-mouse IgG (Sigma B8520, USA) and biotinylated rat anti-mouse IgA (Sigma LO-MA-10, USA) Abs were used for detection. Revelation was performed as described above for human Igs.

Staining quantification was carried out after digitalization with a x40 objective using the slide scanner SCN400 (Leica microsystems, Germany) and TissueIA software (Leica microsystems, Ireland). Quantification included application of algorithms for each immunostaining (Leica microsystems, Germany).

Multiplexed immunofluorescence using tyramide-signal amplification

We fixed all specimens in 7,5% formalin and embedded them in paraffin wax. Unstained 5µm sections were then cut from formalin-fixed paraffin-embedded (FFPE) blocks for immunofluorescence analysis. FFPE sections were deparaffinized in toluene and rehydrated through a graded series from ethanol to water. Antigen retrieval was performed in citrate buffer (pH 6.0 containing 0.1% of triton) using a pressure cooker at 15 pound-force per square inch (PSI) for 5 minutes. We then blocked the slides by incubation in Bloxall (Vector lab, Burlingame, CA) for 15 min and then by 0.3% hydrogen peroxide in 5% goat serum (C07SA, Bio-Rad, Hercules, CA, USA) for 30 min.

We applied to each slide sequential rounds of staining, each including a 30 min protein blocking with 5% goat serum, followed by a primary antibody incubation diluted in 5% normal goat serum solution, and a 40 minutes long incubation with corresponding SuperBoost™ goat anti-rabbit or anti-mouse poly-horseradish peroxidase-conjugated secondary antibody (Thermo Fisher Scientific, Waltham, MA, USA). Each HRP-

Copyright © 2018 by the American Thoracic Society

AJRCCM Articles in Press. Published on 19-October-2018 as 10.1164/rccm.201802-0352OC

conjugated polymer mediated the focal covalent binding to the tissue of a fluorophore using tyramide signal amplification. Finally, this covalent reaction was followed by additional stripping steps in heated citric acid buffer (pH 6.0) with pressure cooker. After the sequential reactions, sections were counterstained with Hoechst (Thermo Fisher Scientific) diluted at 1:500 in TBS-BSA 5% and mounted with Dako fluorescence mounting medium (Dako, Carpinteria, CA). We performed four staining rounds for the first experiment (IL-21 (Merck-Millipore, 06-1074), BCL-6 (Acris, AM33123PUM), CXCR5 (Abcam, AB46218), CD3 (Cell Signaling, 85061S)), and three rounds for the second experiment (CD3, IL-21 and RORγt (Sigma, MABF81)). For negative controls, we used rabbit or mouse isotype controls at the same concentration as the corresponding primary antibodies in 5% normal goat serum.

Finally, stained slides were scanned with the Pannoramic 250 Flash digital microscope (P250 Flash digital microscopes; 3DHISTECH, Budapest, HU).

RNA extraction and RT-qPCR. Total RNA was isolated from lung tissues using the Rneasy® Plus Mini kit (Qiagen, Hilden, Germany). Total RNA (500 ng per sample) was reverse-transcribed and the expression levels in lung tissues of human IL-6 and IL-21 were assessed and reported to those of RPS18, RNA18S and GAPDH housekeeping genes (by using the geometric mean of the three housekeeping genes, HKG); as well as mouse IgA and IgG1 that were reported to those of RNA18S housekeeping gene. The quantification was made by real time quantitative PCR using the iCycler IQ5 PCR (Bio-Rad, Hercules, CA, USA). Data analysis was performed using Bio-Rad iQ5 Software (Bio-Rad, USA).

Copyright © 2018 by the American Thoracic Society

Statistical analysis. Differences between groups were analysed using non-parametric Mann-Whitney U test for unpaired data and Wilcoxon test for paired data. Kruskal-Wallis test (followed by Dunn's test) was used for multiple comparisons. Correlations were assessed by the Spearman's correlation test. A probability value less than 0.05 was considered as statistically significant. Statistical analyses were performed using GraphPad Prism (version 5.00 for Windows; GraphPad Software, San Diego CA; www.graphpad.com).

Ethical considerations. All patients gave signed informed consent to the study protocol, which was approved by our local Ethical committee of Cliniques UCL St-Luc (Ref. #2007/19MARS/58). All animal experiments received approval (Ref. #CEEA34.PRB.135.12) from the ethical review board of Paris Descartes University.

Copyright © 2018 by the American Thoracic Society

AJRCCM Articles in Press. Published on 19-October-2018 as 10.1164/rccm.201802-0352OC

Results

Patient characteristics. Lung tissues were obtained from well-characterized COPD patients (n=34) with various range of airflow limitation and smoking histories, compared to controls (never, former or current smokers) without the disease (i.e., with normal lung function, n=37) (Table 1).

B cells and LF in COPD lung. We first analysed the number of B cells in the airways from controls versus COPD patients. A significant increase was observed in the percentage of B cells, among total cell number, both in smokers (mild increase, p=0.009 smokers vs non-smokers) and in severe COPD patients (p=0.0005 severe COPD vs non-smokers) (Figure 1A and 1B). B cells were negatively correlated with airway obstruction in terms of FEV1 (Figure 1D) and FEV1/FVC ratio (r_s= -0.25, p= 0.03 and r_s= -0.34, p= 0.005). In those CD20-stained lung tissue sections, the number of LF was increased in severe COPD patients as compared to non-smokers controls (p=0.02) (Figures 1A and 1C). LF numbers were also negatively correlated with FEV1 (r_s= -0.37, p=0.002; Figure 1E). CD20+ lymphoid structures were significantly increased in distal lung tissue from severe COPD patients (p=0.0002), present around bronchioles and within parenchymal tissue, and correlated with FEV1 (r_s=-0.47, p=0.0003) and FEV1/FVC ratio (r_s=-0.42, p=0.001), while it was not significantly increased in proximal tissue (Figure 2). Thus, both B cell and (distal) LF numbers were increased in COPD and correlated to disease severity.

Of note, only half (47%) of LF displayed CD21+ follicular DCs (appearing in clusters) and those CD21+ LF numbers were not significantly increased in COPD (Figure E1).

Copyright © 2018 by the American Thoracic Society

Follicular IgA expression in COPD lung. We next characterized Ig expression by B cells from those LF. Most follicular B cells were IgM+ (~70-80%), showing no difference between COPD and control groups (Figure 3). In contrast, a significant increase in follicular IgA+ B cells was observed in severe COPD as compared to controls (~2-fold, 45% vs 25% of follicular cells, p=0.04; and p=0.02 for staining intensity), while no difference was globally observed in IgG+ nor IgM+ B cells (Figure 3). When considering separately proximal and distal airways, IgA upregulation was only significantly observed in distal/parenchymal LF (Figures E2-E3). Moreover, IgA+ cells in distal LF were negatively correlated with airway obstruction in terms of FEV1/FVC ratio (r_s= -0.48, p= 0.001; Figure E3H).

Follicular IgA expression following mice lung infection by Pseudomonas aeruginosa. We then evaluated whether lung infection could underlie an upregulation of follicular IgA expression in the lung, by assessing *Pseudomonas aeruginosa* (PAO-1)-infected mice as an *in vivo* model of chronic lung infection which displays robust peribronchial lymphoid neogenesis within 14 days. First, the global number of (extrafollicular) IgA+ B cells increased at day 28 post-infection (Figure 4D-E). Second, the percentage of IgA+ B cells within LF from those mice tended to increase from day 14 (30±14%) to day 28 post-infection (40±19%) (p=0.06, Figure 4F), while that of IgG+ B cells (which are globally more numerous than IgA) did not change (54±23% at d14, 54±20% at d28) (Figure E4F). Of note, the diffuse alveolar IgG staining likely represents circulating IgG (Figure E4B-C). Accordingly, total IgA and PAO1-specific IgA levels consistently increased in the BALF from infected mice (Figure 4G-H), whereas total IgG did not change and only a few mice mounted a specific IgG response (Figure E4G-H). At the gene level, increased

Copyright © 2018 by the American Thoracic Society

AJRCCM Articles in Press. Published on 19-October-2018 as 10.1164/rccm.201802-0352OC

synthesis of IgG1 (p=0.04) and a trend for increased synthesis of IgA (p=0.12) were observed (Figure 4I and Figure E4I).

Follicular IgA expression in mice following cigarette smoke exposure. The cigarette smoke-induced COPD model was used to assess the effect of chronic smoke exposure on IgA production, including in lymphoid follicles that are observed in this 12-weeks model. No effect was observed on both extrafollicular and follicular IgA stainings, or on BAL IgA content (Figure E5). Similar findings were observed for IgG (Figure E5).

Regulation of IgA production by B cells. In order to link our findings in the COPD lung and this animal model, we assessed *in vitro* whether gram negative-derived LPS or cigarette smoke (CS) could directly regulate normal blood B cells for IgA production. First, no significant cytotoxicity was observed in these conditions, according to PI staining (Figure 5C). Very significant increases in B cell proliferation and survival were observed upon CSE exposure (Figure 5C-5D), while no effect was observed on IgA or IgG production (Figure 5A-5B). Therefore, we evaluated whether relevant immune factors could regulate IgA production, and assessed IL-21 as first candidate (23). We found that B cells stimulated by IL-21 did upregulate IgA production (~ 2 to 5 median fold increase), as well as IgG (~ 10 to 25 fold) and to a lesser extent IgM (~2 fold), irrespectively of CD40L ligation (Figure 6E-G)

Production of IL-21 by follicular Th17 cells in the COPD lung. We also assessed whether follicular IgA upregulation could be associated with local expression of IL-21 or with IL-6, known as cytokines promoting IgA production. Whereas gene expression of IL-6 or IL-21 was not significantly affected (data not shown), intra-follicular numbers of IL-21-expressing cells were significantly up-regulated in mild and severe COPD, as

Copyright © 2018 by the American Thoracic Society

compared to controls (p=0.03 and 0.01 respectively) (Figure 6A-6B). To further confirm the nature of the intra-follicular IL-21+ cells, we performed colocalization by immunofluorescence staining of IL-21 with CD4, Bcl-6 and CXCR5 as markers of follicular Th cells (Tfh) (24). We found that almost all IL-21 producing cells were CD3+, with a few co-expressing CXCR5 and Bcl6, as defined as Tfh (Figure 6C). We next assessed whether IL-21 could be alternatively produced by Th17 cells (25). By dual staining for CD3 and RORγt, we found that a more substantial number of RORγt+ T cells (RORγt+ CD3- cells corresponding to innate lymphocytes) do express IL-21, indicating that Th17 cells were a more prominent source of this cytokine than Tfh but also that IL-21 is expressed by several other, uncharacterized T cells in COPD lymphoid follicles.

Copyright © 2018 by the American Thoracic Society

AJRCCM Articles in Press. Published on 19-October-2018 as 10.1164/rccm.201802-0352OC

Discussion

This study is to our knowledge the first to explore the functional status (in particular Ig production) of B cells within the lymphoid follicles found in the diseased human lung. Our data show that lymphoid aggregates that accumulate preferentially in distal areas of the lung, around bronchioles and in parenchyma, from severe COPD contain B cells that have preferentially switched to IgA. We also show that this follicular IgA response is reproduced in the lungs from mice following Pseudomonas infection, but not following cigarette smoke exposure. Moreover, the follicular IgA expression associates with the presence of T cells expressing IL-21, which is very potent in stimulating IgA and IgG production in vitro, while cigarette smoke directly increases (*in vitro*) the proliferation and survival of B cells but not IgA production.

The presence of LF has been described in several lung diseases such as COPD, cystic fibrosis, bronchiectasis, idiopathic pulmonary fibrosis, pulmonary hypertension, or lung cancer. In lung cancer, those LF (named tumor-induced bronchus-associated lymphoid tissue, Ti-BALT) (26) consist of DC-Lamp+ mature DCs and T cell clusters adjacent to B-cell follicles, and are associated with a better outcome and anti-tumoral responses (27, 28). In COPD, our study confirms that the formation of LF occurs preferentially in distal airways and correlates with disease severity. It was also shown that these LF contain germinal centers, indicating induction of Ig switching (5). Our data further show that this switching concerns IgA, which is the only isotype clearly upregulated within COPD LF while IgG is not significantly affected.

It has been shown that mechanisms of lymphoid neogenesis in COPD involve CXCL13 (9, 10), BAFF (11, 12), IL-17F and IL-17A (13, 29) as well as CXCR3 ligands (14). We

Copyright © 2018 by the American Thoracic Society

and others demonstrated an upregulation of BAFF and APRIL in lungs of smokers and more significantly in COPD lung (11, 12, 15, 30). Frija-Masson et al., showed that the airway epithelium from mice infected with PA expresses IL17A (as well as CXCL12 and CXCL13) (21), further suggesting a role for the airway epithelium in LF neogenesis. It was also shown in mouse models that smoke-induced pulmonary LF persist even after cigarette exposure cessation (31) and were associated with impaired immune responses to bacterial infection (32). Altogether, these data suggest that cigarette smoke and infection could both play roles in LF formation in COPD. However, regarding IgA, this study shows that LFs from smoking mice do not display upregulated IgA (or IgG) production, as confirmed in vitro in cultures of CSE-exposed human B cells. The possibility of combined effects of cigarette smoke and infection should be further studied to better understand the regulation of IgA production in the COPD lung.

The pathways underlying the selective induction of IgA synthesis in COPD-related LF remain uncertain but could consist of epithelial BAFF and T cell-derived IL-21 as first candidates. Thus, besides increased BAFF we found increased IL-21 expression produced by T cells from those LF. It was previously demonstrated that IL-21 has a predominant role for IgA production (23, 33). In addition, lung LF seen in patients with idiopathic pulmonary arterial hypertension patients were also associated with IL-21-producing Tfh together with activation-induced cytidine deaminase (AID) and long-lived CD138+ plasma cells (34), suggesting that LF present in different chronic lung diseases represent local niches of active antibody production. In our COPD study, very few of these IL-21-producing T cells consisted of Tfh cells, whereas a more substantial signal was found in Th17 cells which represent another source of this cytokine (25) and which are reportedly

Copyright © 2018 by the American Thoracic Society

AJRCCM Articles in Press. Published on 19-October-2018 as 10.1164/rccm.201802-0352OC

increased in COPD (35). IL-21+ Th17 cells were also observed in the smoking mice model, where they correlated with activated CD8+ T cells (36). However, IL-21 appeared expressed by several other T cells in our COPD LFs, that further studies should characterize, with NKT cells or Th2 cells representing potential candidates. Of note, only half (47%) of LF from COPD lungs displayed evidence of CD21+ follicular DCs, which thus suggests that they are not mandatory to support COPD lymphoid neogenesis. This was also reported in the model of mice infected by repeated instillations of (heat inactivated) PA that developed LF lacking fDCs (37).

Although the objective quantification of IHC staining using color deconvolution represents a strength of this work, one limitation relates to the fact that our results were not extrapolated to whole lung distribution such as described in the ATS/ERC guidelines (38), as quantification of Ig expressing cells (or Ig-stained area) were performed on the lymphoid structures of whole sections for each mouse lung or human biopsy. Another limitation is the fact that a role of inhaled corticosteroids cannot be excluded, as most severe COPD patients were under this treatment, even though this seems unlikely as already reported for polymeric Ig receptor expression (39). Only some severe COPD displayed increased B cell and LF numbers, but we could not relate this to any clinical feature, due to absence of exacerbation data in this series and to modest effective, except that it was clearly independent from active smoking as all severe COPD patients were ex-smokers except one. The fact that IgA upregulation more selectively concerns distal, and not proximal, follicles should also deserve further studies; one could speculate that it could reflect an adaptive IgA response to antigens more selectively present or released in distal areas of the COPD lungs.

Copyright © 2018 by the American Thoracic Society

Altogether our study shows that IgA production occurs in distal (peribronchiolar and parenchymal) LF from severe COPD patients, and that this feature is recapitulated in the lungs from Pseudomonas-infected mice and associates with the induction of follicular IL-21 expression in T cells. Our data also indicate that cigarette smoke could directly promote B cell accumulation in the lung, but without affecting IgA production both in cultured human B cells and in the lungs from smoking mice. It remains to be determined whether this IgA response is protective (e.g., against inhaled pathogens or toxic particles) or harmful (e.g., against autoantigens). A better understanding of the role of this follicular response in COPD, presumably representing a feature of exacerbated mucosal responses against microbial and/or self-antigens, could help to define strategies to restore mucosal immune homeostasis in this disease.

Copyright © 2018 by the American Thoracic Society

AJRCCM Articles in Press. Published on 19-October-2018 as 10.1164/rccm.201802-0352OC

Acknowledgements

The Authors thank the Pathology Department, CHU UCL Namur (Godinne Site), Yvoir, Belgium; the Thoracic Surgery departments of Cliniques universitaires St Luc, Brussels (Pr A. Poncelet) and of CHU UCL Namur (Godinne Site), Yvoir (P. Eucher, B. Rondelet). The Authors also thank B. Marsland (Lausanne, CH) for providing murine IgG1 primers.

Disclosure: The authors state no conflict of interest to declare.

Copyright © 2018 by the American Thoracic Society

References

1. Saetta M, Di Stefano A, Turato G, Facchini FM, Corbino L, Mapp CE, Maestrelli P, Ciaccia A, Fabbri LM. CD8+ T-lymphocytes in peripheral airways of smokers with chronic obstructive pulmonary disease. *American journal of respiratory and critical care medicine* 1998; 157: 822-826.
2. Cosio MG, Guerassimov A. Chronic obstructive pulmonary disease. Inflammation of small airways and lung parenchyma. *American journal of respiratory and critical care medicine* 1999; 160: S21-25.
3. Hogg JC, Chu F, Utokaparch S, Woods R, Elliott WM, Buzatu L, Cherniack RM, Rogers RM, Sciurba FC, Coxson HO, Pare PD. The nature of small-airway obstruction in chronic obstructive pulmonary disease. *The New England journal of medicine* 2004; 350: 2645-2653.
4. Gosman MM, Willemse BW, Jansen DF, Lapperre TS, van Schadewijk A, Hiemstra PS, Postma DS, Timens W, Kerstjens HA. Increased number of B-cells in bronchial biopsies in COPD. *The European respiratory journal* 2006; 27: 60-64.
5. van der Strate BW, Postma DS, Brandsma CA, Melgert BN, Luinge MA, Geerlings M, Hylkema MN, van den Berg A, Timens W, Kerstjens HA. Cigarette smoke-induced emphysema: A role for the B cell? *American journal of respiratory and critical care medicine* 2006; 173: 751-758.
6. Brusselle GG, Demoor T, Bracke KR, Brandsma CA, Timens W. Lymphoid follicles in (very) severe COPD: beneficial or harmful? *The European respiratory journal* 2009; 34: 219-230.
7. Brusselle GG, Joos GF, Bracke KR. New insights into the immunology of chronic obstructive pulmonary disease. *Lancet* 2011; 378: 1015-1026.
8. Yadava K, Marsland BJ. Lymphoid follicles in chronic lung diseases. *Thorax* 2013; 68: 597-598.
9. Bracke KR, Verhamme FM, Seys LJ, Bantsimba-Malanda C, Cunoosamy DM, Herbst R, Hammad H, Lambrecht BN, Joos GF, Brusselle GG. Role of CXCL13 in cigarette smoke-induced lymphoid follicle formation and chronic obstructive pulmonary disease. *American journal of respiratory and critical care medicine* 2013; 188: 343-355.
10. Litsiou E, Semitekolou M, Galani IE, Morianos I, Tsoutsa A, Kara P, Rontogianni D, Bellenis I, Konstantinou M, Potaris K, Andreakos E, Sideras P, Zakynthinos S, Tsoumakidou M. CXCL13 production in B cells via Toll-like receptor/lymphotoxin receptor signaling is involved in lymphoid neogenesis in chronic obstructive pulmonary disease. *American journal of respiratory and critical care medicine* 2013; 187: 1194-1202.
11. Polverino F, Baraldo S, Bazzan E, Agostini S, Turato G, Lunardi F, Balestro E, Damin M, Papi A, Maestrelli P, Calabrese F, Saetta M. A novel insight into adaptive immunity in chronic obstructive pulmonary disease: B cell activating factor belonging to the tumor necrosis factor family. *American journal of respiratory and critical care medicine* 2010; 182: 1011-1019.
12. Seys LJ, Verhamme FM, Schinwald A, Hammad H, Cunoosamy DM, Bantsimba-Malanda C, Sabirsh A, McCall E, Flavell L, Herbst R, Provoost S, Lambrecht BN, Joos GF, Brusselle GG, Bracke KR. Role of B Cell-Activating Factor in

Copyright © 2018 by the American Thoracic Society

AJRCCM Articles in Press. Published on 19-October-2018 as 10.1164/rccm.201802-0352OC

Chronic Obstructive Pulmonary Disease. *American journal of respiratory and critical care medicine* 2015; 192: 706-718.
13. Eustace A, Smyth LJC, Mitchell L, Williamson K, Plumb J, Singh D. Identification of cells expressing IL-17A and IL-17F in the lungs of patients with COPD. *Chest* 2011; 139: 1089-1100.
14. Kelsen SG, Aksoy MO, Georgy M, Hershman R, Ji R, Li X, Hurford M, Solomides C, Chatila W, Kim V. Lymphoid follicle cells in chronic obstructive pulmonary disease overexpress the chemokine receptor CXCR3. *American journal of respiratory and critical care medicine* 2009; 179: 799-805.
15. Ladjemi MZ, Lecocq M, Weynand B, Bowen H, Gould HJ, Van Snick J, Detry B, Pilette C. Increased IgA production by B-cells in COPD via lung epithelial interleukin-6 and TACI pathways. *The European respiratory journal* 2014.
16. Pilette C, Godding V, Kiss R, Delos M, Verbeken E, Decaestecker C, De Paepe K, Vaerman JP, Decramer M, Sibille Y. Reduced epithelial expression of secretory component in small airways correlates with airflow obstruction in chronic obstructive pulmonary disease. *American journal of respiratory and critical care medicine* 2001; 163: 185-194.
17. Polosukhin VV, Cates JM, Lawson WE, Zaynagetdinov R, Milstone AP, Massion PP, Ocak S, Ware LB, Lee JW, Bowler RP, Kononov AV, Randell SH, Blackwell TS. Bronchial secretory immunoglobulin a deficiency correlates with airway inflammation and progression of chronic obstructive pulmonary disease. *American journal of respiratory and critical care medicine* 2011; 184: 317-327.
18. Gohy ST, Detry BR, Lecocq M, Bouzin C, Weynand BA, Amatngalim GD, Sibille YM, Pilette C. Polymeric immunoglobulin receptor down-regulation in chronic obstructive pulmonary disease. Persistence in the cultured epithelium and role of transforming growth factor-beta. *American journal of respiratory and critical care medicine* 2014; 190: 509-521.
19. Wu Y, Bressette D, Carrell JA, Kaufman T, Feng P, Taylor K, Gan Y, Cho YH, Garcia AD, Gollatz E, Dimke D, LaFleur D, Migone TS, Nardelli B, Wei P, Ruben SM, Ullrich SJ, Olsen HS, Kanakaraj P, Moore PA, Baker KP. Tumor necrosis factor (TNF) receptor superfamily member TACI is a high affinity receptor for TNF family members APRIL and BLyS. *The Journal of biological chemistry* 2000; 275: 35478-35485.
20. Cerutti A, Puga I, Cols M. New helping friends for B cells. *European journal of immunology* 2012; 42: 1956-1968.
21. Frija-Masson J, Martin C, Regard L, Lothe MN, Touqui L, Durand A, Lucas B, Damotte D, Alifano M, Fajac I, Burgel PR. Bacteria-driven peribronchial lymphoid neogenesis in bronchiectasis and cystic fibrosis. *The European respiratory journal* 2017; 49.
22. Martin C, Thevenot G, Danel S, Chapron J, Tazi A, Macey J, Dusser DJ, Fajac I, Burgel PR. Pseudomonas aeruginosa induces vascular endothelial growth factor synthesis in airway epithelium in vitro and in vivo. *The European respiratory journal* 2011; 38: 939-946.
23. Avery DT, Bryant VL, Ma CS, de Waal Malefyt R, Tangye SG. IL-21-induced isotype switching to IgG and IgA by human naive B cells is differentially regulated by IL-4. *Journal of immunology* 2008; 181: 1767-1779.

Copyright © 2018 by the American Thoracic Society

24. Velu V, Mylvaganam GH, Gangadhara S, Hong JJ, Iyer SS, Gumber S, Ibegbu CC, Villinger F, Amara RR. Induction of Th1-Biased T Follicular Helper (Tfh) Cells in Lymphoid Tissues during Chronic Simian Immunodeficiency Virus Infection Defines Functionally Distinct Germinal Center Tfh Cells. *Journal of immunology* 2016; 197: 1832-1842.
25. Liu SM, King C. IL-21-producing Th cells in immunity and autoimmunity. *Journal of immunology* 2013; 191: 3501-3506.
26. Dieu-Nosjean MC, Antoine M, Danel C, Heudes D, Wislez M, Poulot V, Rabbe N, Laurans L, Tartour E, de Chaisemartin L, Lebecque S, Fridman WH, Cadranel J. Long-term survival for patients with non-small-cell lung cancer with intratumoral lymphoid structures. *Journal of clinical oncology : official journal of the American Society of Clinical Oncology* 2008; 26: 4410-4417.
27. Germain C, Gnjatic S, Tamzalit F, Knockaert S, Remark R, Goc J, Lepelley A, Becht E, Katsahian S, Bizouard G, Validire P, Damotte D, Alifano M, Magdeleinat P, Cremer I, Teillaud JL, Fridman WH, Sautes-Fridman C, Dieu-Nosjean MC. Presence of B cells in tertiary lymphoid structures is associated with a protective immunity in patients with lung cancer. *American journal of respiratory and critical care medicine* 2014; 189: 832-844.
28. Goc J, Germain C, Vo-Bourgais TK, Lupo A, Klein C, Knockaert S, de Chaisemartin L, Ouakrim H, Becht E, Alifano M, Validire P, Remark R, Hammond SA, Cremer I, Damotte D, Fridman WH, Sautes-Fridman C, Dieu-Nosjean MC. Dendritic cells in tumor-associated tertiary lymphoid structures signal a Th1 cytotoxic immune contexture and license the positive prognostic value of infiltrating CD8+ T cells. *Cancer research* 2014; 74: 705-715.
29. Mori M, Bjermer L, Erjefalt JS, Stampfli MR, Roos AB. Small airway epithelial-C/EBPbeta is increased in patients with advanced COPD. *Respiratory research* 2015; 16: 133.
30. Polverino F, Cosio BG, Pons J, Laucho-Contreras M, Tejera P, Iglesias A, Rios A, Jahn A, Sauleda J, Divo M, Pinto-Plata V, Sholl L, Rosas IO, Agusti A, Celli BR, Owen CA. B Cell-Activating Factor. An Orchestrator of Lymphoid Follicles in Severe Chronic Obstructive Pulmonary Disease. *American journal of respiratory and critical care medicine* 2015; 192: 695-705.
31. Morissette MC, Jobse BN, Thayaparan D, Nikota JK, Shen P, Labiris NR, Kolbeck R, Nair P, Humbles AA, Stampfli MR. Persistence of pulmonary tertiary lymphoid tissues and anti-nuclear antibodies following cessation of cigarette smoke exposure. *Respiratory research* 2014; 15: 49.
32. Lugade AA, Bogner PN, Thatcher TH, Sime PJ, Phipps RP, Thanavala Y. Cigarette smoke exposure exacerbates lung inflammation and compromises immunity to bacterial infection. *Journal of immunology* 2014; 192: 5226-5235.
33. Bryant VL, Ma CS, Avery DT, Li Y, Good KL, Corcoran LM, de Waal Malefyt R, Tangye SG. Cytokine-mediated regulation of human B cell differentiation into Ig-secreting cells: predominant role of IL-21 produced by CXCR5+ T follicular helper cells. *Journal of immunology* 2007; 179: 8180-8190.
34. Perros F, Dorfmuller P, Montani D, Hammad H, Waelput W, Girerd B, Raymond N, Mercier O, Mussot S, Cohen-Kaminsky S, Humbert M, Lambrecht BN.

Copyright © 2018 by the American Thoracic Society

AJRCCM Articles in Press. Published on 19-October-2018 as 10.1164/rccm.201802-0352OC

Pulmonary lymphoid neogenesis in idiopathic pulmonary arterial hypertension. *American journal of respiratory and critical care medicine* 2012; 185: 311-321.

35. Di Stefano A, Caramori G, Gnemmi I, Contoli M, Vicari C, Capelli A, Magno F, D'Anna SE, Zanini A, Brun P, Casolari P, Chung KF, Barnes PJ, Papi A, Adcock I, Balbi B. T helper type 17-related cytokine expression is increased in the bronchial mucosa of stable chronic obstructive pulmonary disease patients. *Clinical and experimental immunology* 2009; 157: 316-324.
36. Duan MC, Huang Y, Zhong XN, Tang HJ. Th17 cell enhances CD8 T-cell cytotoxicity via IL-21 production in emphysema mice. *Mediators Inflamm* 2012; 2012: 898053.
37. Fleige H, Ravens S, Moschovakis GL, Bolter J, Willenzon S, Sutter G, Haussler S, Kalinke U, Prinz I, Forster R. IL-17-induced CXCL12 recruits B cells and induces follicle formation in BALT in the absence of differentiated FDCs. *The Journal of experimental medicine* 2014; 211: 643-651.
38. Hsia CC, Hyde DM, Ochs M, Weibel ER, Structure AEJTFoQAoL. An official research policy statement of the American Thoracic Society/European Respiratory Society: standards for quantitative assessment of lung structure. *American journal of respiratory and critical care medicine* 2010; 181: 394-418.
39. Ladjemi M, Gras D, Gohy S, Chanez P, Pilette C. Reply to: The Bronchial Epithelial Secretory IgA System in Asthma. *American journal of respiratory and critical care medicine* 2018.

Copyright © 2018 by the American Thoracic Society

Tables

Table 1. Patients' characteristics of the study population.

	Controls		COPD	
	Non-smokers	**Smokers**	**GOLD I-II**	**GOLD III-IV**
N subjects	21	13	19	18
Age (years, mean ± SD)	51.8 ± 18.8	59.2 ± 11.4	64.8 ± 11.8 *	56.9 ± 6.1
Gender (Male/Female)	8/13	7/6	14/5	11/7
Smokers, n (ex-/current) ***	0	13 (6/7)	19 (9/10)	18 (17/1)
Smoking (PY, N=65)	0	46.1 ± 26.5 ***	47.4 ± 21.4 ***	45.3 ± 23.3 ***
Postβ2 FEV1 (% pred, N=69)	92.6 ± 18.2	95.4 ± 12.7 §§§	80.6 ± 14.8 †††	21.6 ± 7.3 ***
FEV1/FVC (%, N=66)	86.7 ± 13.8	76.8 ± 4.5 §§§	63.7 ± 6.4 ***	34.2 ± 10.3 ***
DLCO (% pred, N=55)	79.4 ± 12.4	73.5 ± 11.3 §§§	58.2 ± 15.1 *†	26.8 ± 10.2 ***
Inhaled corticosteroids, n ***	0	0	3	17

Demographic data, lung function tests and smoking history are stated for the patient groups, classified according to smoking history and the presence of airflow limitation. Values represent mean ± SD. Definition of abbreviations: FEV1: Forced Expiratory Volume in one sec.; FVC: Forced Vital Capacity; DLCO: Diffusing capacity of carbon monoxide; % pred: percent predicted. Eight very severe COPD patients were also treated by maintenance oral steroids (4 to 8 mg methylprednisolone).

** p<0.05, ** p<0.01 and *** p<0.001 (for comparisons versus control non smokers); § p<0.05, §§ p<0.01 and §§§ p<0.001 (for comparisons versus control smokers); † p<0.05, †† p<0.01 and ††† p<0.001 (for comparisons of mild versus severe COPD). Kruskal-*

Copyright © 2018 by the American Thoracic Society

AJRCCM Articles in Press. Published on 19-October-2018 as 10.1164/rccm.201802-0352OC

Wallis test and Dunn's comparison tests were used for multiple comparisons. Chi-square test was used to compare gender, smoking and treatment (by inhaled corticosteroids) status.

Copyright © 2018 by the American Thoracic Society

Figure legends

Figure 1: CD20 staining in human lung tissue (A) Representative CD20 staining (brown) and hematoxylin counterstaining (blue) in lung tissues from one control non-smoker, one smoker, one GOLD II and one GOLD IV COPD patient, and non-immune control IgG staining, and evaluation of **(B)** the percentage of CD20 positive B cells among total cells, and **(C)** the number of CD20 positive lymphoid follicles per tissue area in whole lung tissue sections. Among controls (n=34), non-smokers are represented by white circles, control ex-smokers and current smokers by white and black triangles, respectively. Among COPD patients (n=37), white squares represent ex-smokers with GOLD I-II COPD and black squares active smokers with GOLD I-II COPD patients; white inverted triangles represent ex-smokers with GOLD III-IV COPD and black inverted triangles smokers with GOLD III-IV COPD. Correlation of CD20+ B cells (D) and LF (E) with FEV1 values in all groups. Scale bar, 100μm. Lines represent median and interquartile range. Mann-Whitney U test for comparisons and Spearman test for correlation; * $p<0.05$, ** $p<0.01$, *** $p<0.001$.

Figure 2: CD20 positive lymphoid follicles (LF) in proximal and distal lung tissue (A) Representative peri-bronchial LF in a GOLD IV COPD patient, and evaluation of **(B)** the number of CD20 positive LF per tissue area in large airways. **(C)** Representative parenchymal LF in a GOLD IV COPD patient, and evaluation of **(D)** the number of CD20 positive LF per tissue area in small airways. **(E)** Correlation of distal LF with FEV1 values in all groups. Scale bar, 100μm. Lines represent median and interquartile range. Mann-Whitney U test for comparisons and Spearman test for correlation; ***$p<0.001$.

Copyright © 2018 by the American Thoracic Society

AJRCCM Articles in Press. Published on 19-October-2018 as 10.1164/rccm.201802-0352OC

Figure 3: Intra-follicular immunoglobulin expression in lung tissue. (A), (B) and **(C)** Representative IgA, IgG and IgM stainings (brown) and hematoxylin counterstaining (blue) within a lymphoid structure. Evaluation of **(D), (E)** and **(F)** the number of intra-follicular IgA, IgG or IgM positive cells (% of intra-follicular total cells) and **(G), (H)** and **(I)** the staining per LF surface area of intra-follicular IgA, IgG or IgM (thus reported to the lymphoid structure surface area). Scale bar, 100µm. Lines represent median and interquartile range. Mann-Whitney U test; * $p<0.05$; **$p<0.01$.

Figure 4: IgA expression in lung tissue and broncho-alveolar lavage from Pseudomonas infected mice. (A), **(B)** and **(C)** Representative IgA staining (brown) and hematoxylin counterstaining (blue) in lung tissue from non-immune control IgG staining, mice instilled with sterile beads or PAO1-infected mice, respectively; and evaluation of **(D)** and **(E)** total IgA expression and **(F)** intra-follicular IgA-positive cells at days 14 and 28 post-infection; **(G)** and **(H)** total and PAO-specific IgA in broncho-alveolar lavage from mice instilled with sterile beads or PAO-infected mice at day 14 post-infection; **(I)** IgA mRNA expression corrected to the housekeeping gene in lung tissue from mice instilled with sterile beads or PAO-infected mice at day 14 post-infection. White circles (mice instilled with sterile beads, n=5 to 9) and black circles (mice infected with PAO beads, n=5 to 10). Scale bar, 100µm. Lines represent median and interquartile range. Mann-Whitney U test; * $p<0.05$, ** $p<0.01$.

Figure 5: Effect of LPS or cigarette smoke exposure on human B cell Ig production, survival and proliferation. Blood B cells were assessed by flow cytometry for cell survival and proliferation and cell-free supernatants were assessed by ELISA for IgA (**A**) and IgG (**B**)following culture for 13 days in resting or in LPS- or CSE- stimulated

Copyright © 2018 by the American Thoracic Society

conditions. **(C)** Percentage of viable B cells (PI negative cells), **(D)** Percentage of proliferating B cells as measured by CFSE staining. (**A-G**) IgA, IgG (F) and IgM (G) production by B cells stimulated by IL-21, CD40L or both (and expressed as fold change from unstimulated control cells). Lines represent median and interquartile range of data from 23 to 27 independent cultures/donors. Wilcoxon paired test *p<0.05, *** p<0.001.

Figure 6: IL-21 staining in lung tissue and co-localization with T cells. (A) Representative IL-21 staining (red) in lung tissue from a patient with COPD, and (B) evaluation of the number of intra-follicular IL-21$^+$ cells in controls (8 non-smokers and 6 smokers), GOLD I-II and GOLD III-IV COPD patients. Lines represent mean ± SD. Mann-Whitney U test ; *p<0.05. (C) Representative co-staining of IL-21 (orange) with CD3 (red), Bcl-6 (yellow) and CXCR5 (green), performed by multiplexed immunofluorescence using tyramide-signal amplification. We used Hoechst (blue) for nuclear counterstaining. (D) Representative co-staining of IL-21 (orange) with CD3 (red), and RORγt (green), performed by multiplexed immunofluorescence using tyramide-signal amplification. We used Hoechst (blue) for nuclear counterstaining.

Copyright © 2018 by the American Thoracic Society

AJRCCM Articles in Press. Published on 19-October-2018 as 10.1164/rccm.201802-0352OC

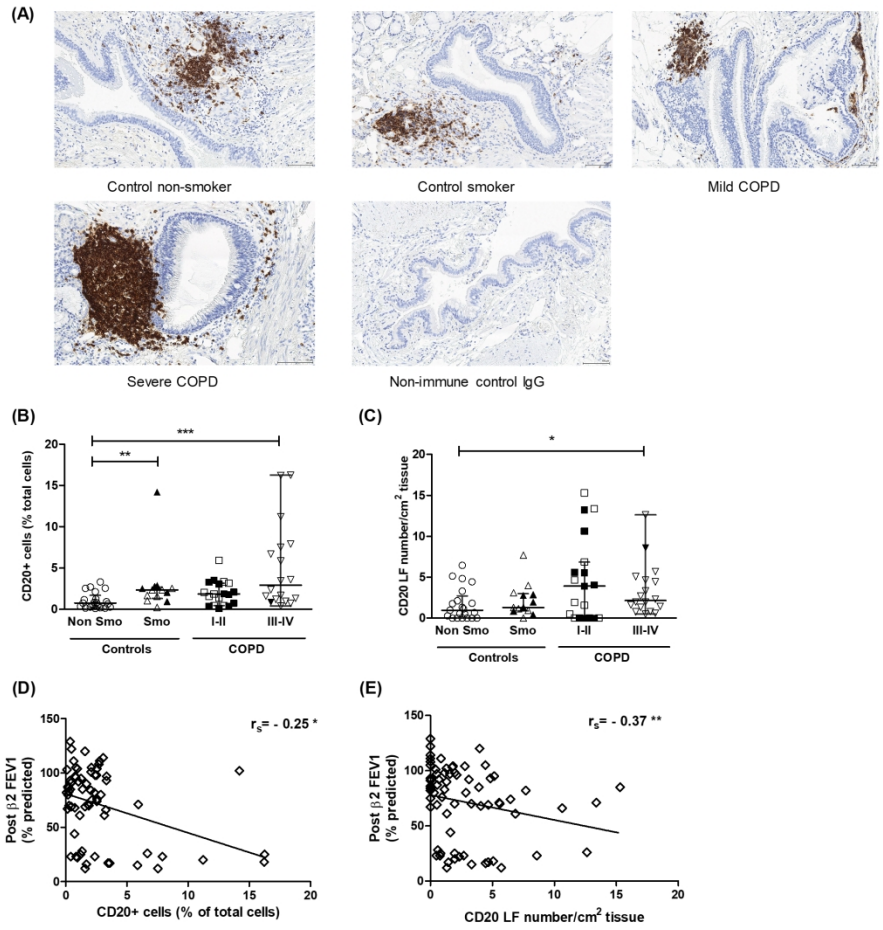

Figure 1

Figure 1: CD20 staining in human lung tissue (A) Representative CD20 staining (brown) and hematoxylin counterstaining (blue) in lung tissues from one control non-smoker, one smoker, one GOLD II and one GOLD IV COPD patient, and non-immune control IgG staining, and evaluation of (B) the percentage of CD20 positive B cells among total cells, and (C) the number of CD20 positive lymphoid follicles per tissue area in whole lung tissue sections. Among controls (n=34), non-smokers are represented by white circles, control ex-smokers and current smokers by white and black triangles, respectively. Among COPD patients (n=37), white squares represent ex-smokers with GOLD I-II COPD and black squares active smokers with GOLD I-II COPD patients; white inverted triangles represent ex-smokers with GOLD III-IV COPD and black inverted triangles smokers with GOLD III-IV COPD. Correlation of CD20+ B cells (D) and LF (E) with FEV1 values in all groups. Scale bar, 100μm. Lines represent median and interquartile range. Mann-Whitney U test for comparisons and Spearman test for correlation; * $p<0.05$, ** $p<0.01$, *** $p<0.001$.

190x254mm (300 x 300 DPI)

Copyright © 2018 by the American Thoracic Society

AJRCCM Articles in Press. Published on 19-October-2018 as 10.1164/rccm.201802-0352OC

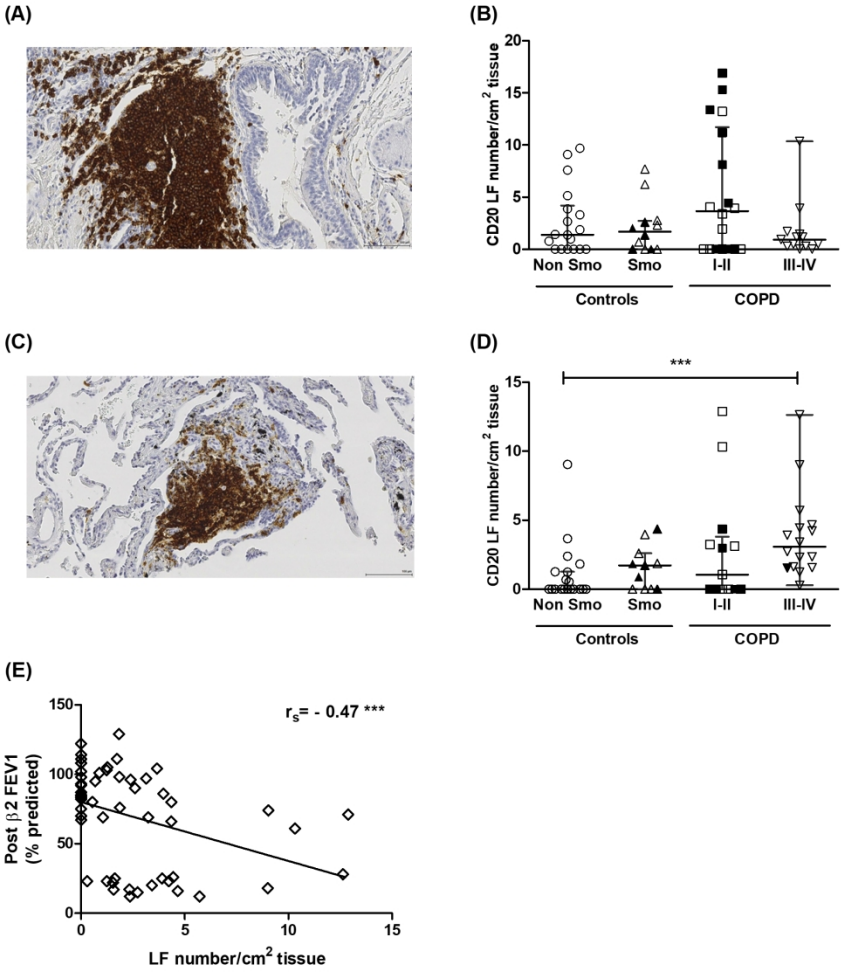

Figure 2

Figure 2: CD20 positive lymphoid follicles (LF) in proximal and distal lung tissue (A) Representative peri-bronchial LF in a GOLD IV COPD patient, and evaluation of (B) the number of CD20 positive LF per tissue area in large airways. (C) Representative parenchymal LF in a GOLD IV COPD patient, and evaluation of (D) the number of CD20 positive LF per tissue area in small airways. (E) Correlation of distal LF with FEV1 values in all groups. Scale bar, 100μm. Lines represent median and interquartile range. Mann-Whitney U test for comparisons and Spearman test for correlation; ***p<0.001.

190x254mm (300 x 300 DPI)

Copyright © 2018 by the American Thoracic Society

AJRCCM Articles in Press. Published on 19-October-2018 as 10.1164/rccm.201802-0352OC

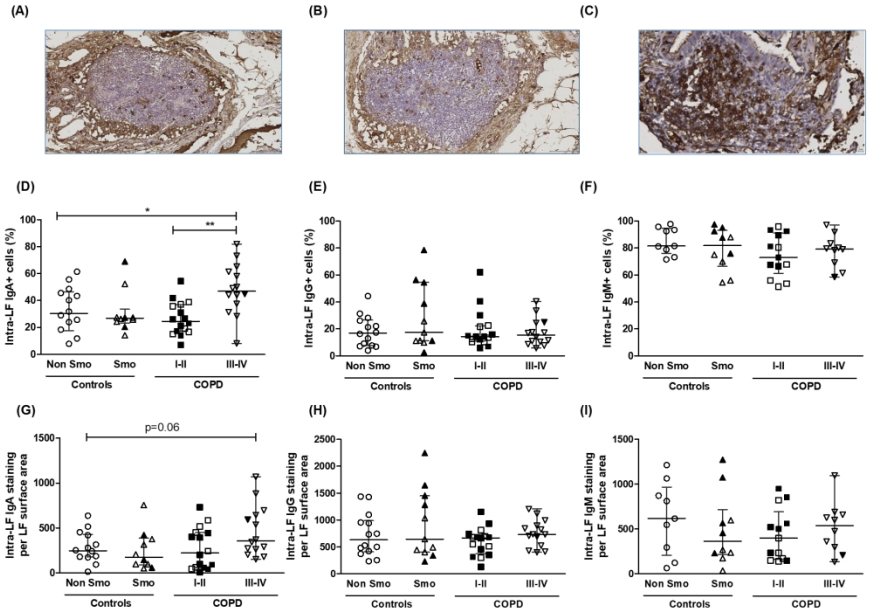

Figure 3

Figure 3: Intra-follicular immunoglobulin expression in lung tissue. (A), (B) and (C) Representative IgA, IgG and IgM stainings (brown) and hematoxylin counterstaining (blue) within a lymphoid structure. Evaluation of (D), (E) and (F) the number of intra-follicular IgA, IgG or IgM positive cells (% of intra-follicular total cells) and (G), (H) and (I) the staining per LF surface area of intra-follicular IgA, IgG or IgM (thus reported to the lymphoid structure surface area). Scale bar, 100µm. Lines represent median and interquartile range. Mann-Whitney U test; * $p<0.05$; ** $p<0.01$.

190x254mm (300 x 300 DPI)

Copyright © 2018 by the American Thoracic Society

AJRCCM Articles in Press. Published on 19-October-2018 as 10.1164/rccm.201802-0352OC

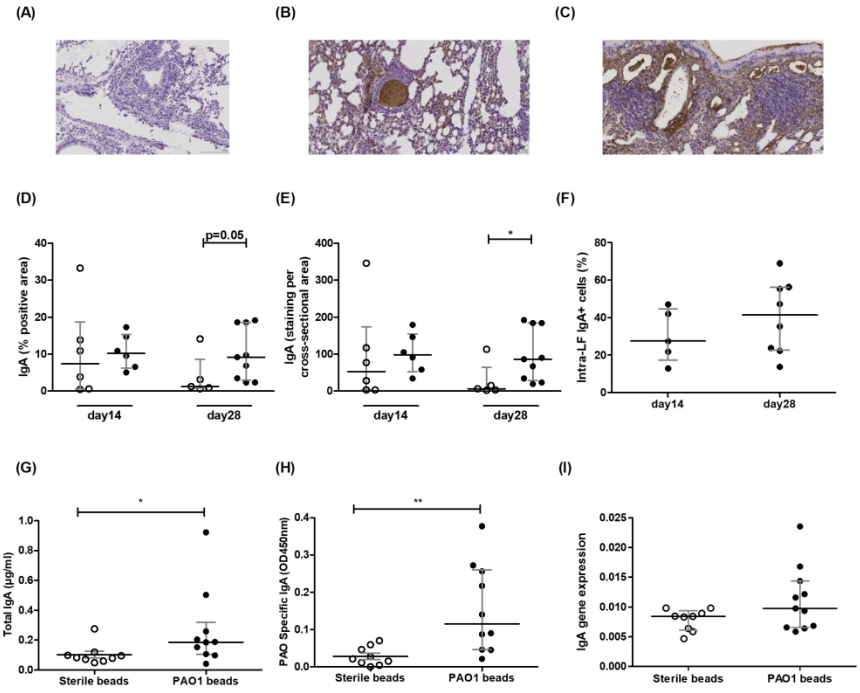

Figure 4

Figure 4: IgA expression in lung tissue and broncho-alveolar lavage from Pseudomonas infected mice. (A), (B) and (C) Representative IgA staining (brown) and hematoxylin counterstaining (blue) in lung tissue from non-immune control IgG staining, mice instilled with sterile beads or PAO1-infected mice, respectively; and evaluation of (D) and (E) total IgA expression and (F) intra-follicular IgA-positive cells at days 14 and 28 post-infection; (G) and (H) total and PAO-specific IgA in broncho-alveolar lavage from mice instilled with sterile beads or PAO-infected mice at day 14 post-infection; (I) IgA mRNA expression corrected to the housekeeping gene in lung tissue from mice instilled with sterile beads or PAO-infected mice at day 14 post-infection. White circles (mice instilled with sterile beads, n=5 to 9) and black circles (mice infected with PAO beads, n=5 to 10). Scale bar, 100µm. Lines represent median and interquartile range. Mann-Whitney U test; * $p<0.05$, ** $p<0.01$.

190x254mm (300 x 300 DPI)

Copyright © 2018 by the American Thoracic Society

AJRCCM Articles in Press. Published on 19-October-2018 as 10.1164/rccm.201802-0352OC

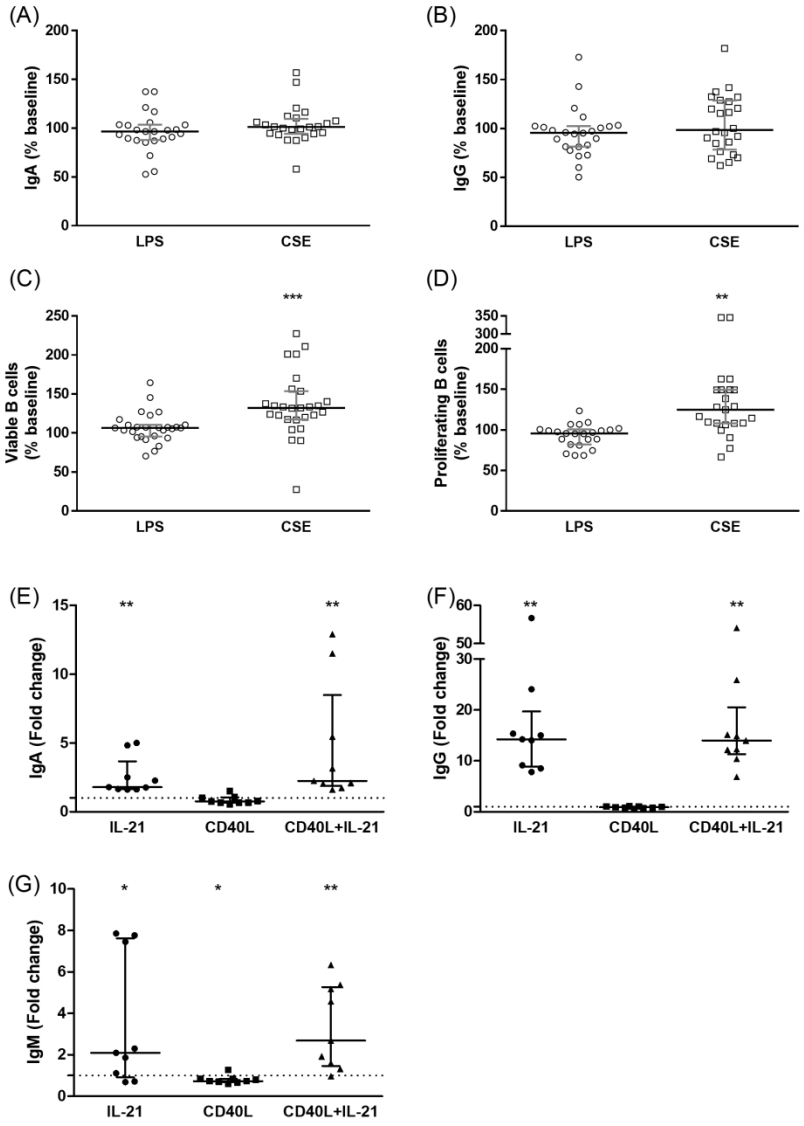

Figure 5

Figure 5: Effect of LPS or cigarette smoke exposure on human B cell Ig production, survival and proliferation. Blood B cells were assessed by flow cytometry for cell survival and proliferation and cell-free supernatants were assessed by ELISA for IgA (A) and IgG (B)following culture for 13 days in resting or in LPS- or CSE- stimulated conditions. (C) Percentage of viable B cells (PI negative cells), (D) Percentage of proliferating B cells as measured by CFSE staining. (A-G) IgA, IgG (F) and IgM (G) production by B cells stimulated by IL-21, CD40L or both (and expressed as fold change from unstimulated control cells). Lines represent median and interquartile range of data from 23 to 27 independent cultures/donors. Wilcoxon paired test *p<0.05, *** p<0.001.

190x254mm (300 x 300 DPI)

Copyright © 2018 by the American Thoracic Society

AJRCCM Articles in Press. Published on 19-October-2018 as 10.1164/rccm.201802-0352OC

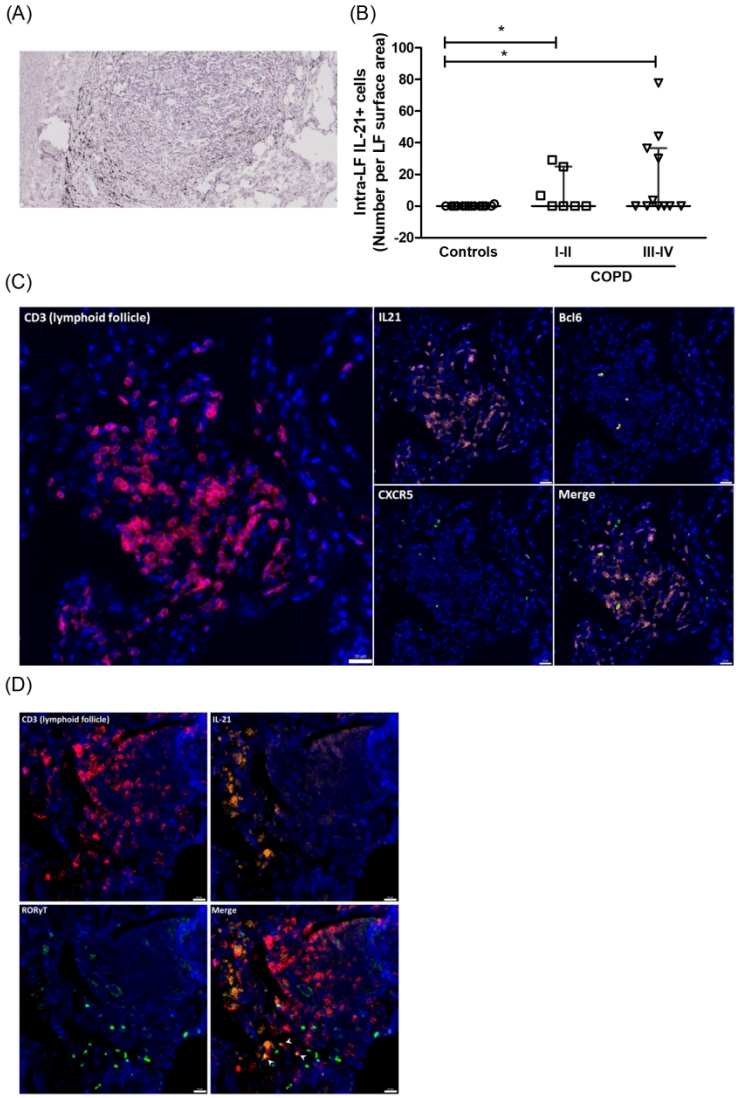

Figure 6

Figure 6: IL-21 staining in lung tissue and co-localization with T cells. (A) Representative IL-21 staining (red) in lung tissue from a patient with COPD, and (B) evaluation of the number of intra-follicular IL-21+ cells in controls (8 non-smokers and 6 smokers), GOLD I-II and GOLD III-IV COPD patients. Lines represent mean ± SD. Mann-Whitney U test ; *p<0.05. (C) Representative co-staining of IL-21 (orange) with CD3 (red), Bcl-6 (yellow) and CXCR5 (green), performed by multiplexed immunofluorescence using tyramide-signal amplification. We used Hoechst (blue) for nuclear counterstaining. (D) Representative co-staining of IL-21 (orange) with CD3 (red), and RORγt (green), performed by multiplexed immunofluorescence using tyramidesignal amplification. We used Hoechst (blue) for nuclear counterstaining.

190x254mm (300 x 300 DPI)

Copyright © 2018 by the American Thoracic Society

AJRCCM Articles in Press. Published on 19-October-2018 as 10.1164/rccm.201802-0352OC

Supplemental material:

In vivo model of persistent lung infection with Pseudomonas aeruginosa. Mice were infected as previously described (22). Briefly, sterile agarose beads and agarose beads coated with the PA strain PAO1 (inoculum containing mean±sem $6\times10^5 \pm 3\times10^5$ cfu/mouse; median size of the beads, 300 μm) were instilled through a cannula into the mice trachea. Mice were sacrificed at day 14 or 28. For histological analysis, lungs were removed after flushing 4% paraformaldehyde through the right heart, were fixed in 4% paraformaldehyde and embedded in paraffin; 5-μm sections were prepared for IHC. Bronchoalveolar lavage (BAL) was also harvested at day 14 post-infection.

In vivo model of COPD upon cigarette smoke exposure. CS-treated animals were exposed to 6 cigarettes (3R4F research cigarettes with filter, Kentucky Tobacco Research and Development Center, University of Kentucky) twice a day for 12 weeks (5 days/week), in a nose-only smoke-exposure system (InExpose System, Scireq). Control mice were exposed to ambient air for the same duration. At sacrifice, BAL was performed in mice anesthetized with a mixture of ketamine (150 mg/kg) and xylazine (10 mg/kg) and tracheotomized before heart-left lung block removal, fixation in 6% paraformaldehyde at a constant hydrostatic pressure of 25cm H_2O for 24h, and embedding in paraffin to assess Ig's in lymphoid aggregates.

Human B cell isolation and stimulation. Leucocytes were isolated from buffy coats of healthy blood donors by centrifugation of whole blood for 20 minutes. PBMCs were then isolated using centrifugation on a Lymphoprep gradient for 20 minutes. Blood B cells were separated by magnetic cell sorting using CD19+ microbeads (Miltenyi Biotec), and cultured in the presence or not of LPS (1 μg/ml), cigarette smoke extract (5%), IL-21 (50 ng/ml; kind gift from L. Dumoutier, UCL, Brussels, Belgium), and/or CD40 ligand through irradiated 3T6-CD40L cells (100,000 cells/well; kind gift from Pr. P. Van der Bruggen, UCL, Brussels, Belgium). Cell-free supernatants were harvested at day 6 and day 13 for Ig's detection by ELISA and B cells were

Copyright © 2018 by the American Thoracic Society

AJRCCM Articles in Press. Published on 19-October-2018 as 10.1164/rccm.201802-0352OC

harvested for viability or proliferation studies respectively by staining with propidium iodide (PI) or carboxyfluorescein succinimidyl ester (CFSE) as previously described (15).

Immunohistochemistry (IHC). Serial lung sections of 5-µm thickness were cut from paraffin blocks, spread on polylysine-coated glass slides, and dried at 37°C for at least 24 h. The slides were then processed for IHC; each step of the procedure being followed by washing with Tris-buffered saline (pH 7.4). CD20 and CD21 stainings were performed using the Benchmark XT machine (Roche, Switzerland). The specimens were incubated overnight at 4°C with *ready-to-use* mouse anti-human CD20 mAb (Clone L26) (Dako, Denmark) or rabbit anti-human CD21 mAb (Clone EP64) (BioSB, USA), respectively revealed with the Ultra View Universal DAB or Alkaline Phosphatase Red detection kits (Roche, Switzerland) according to the manufacturer's instructions. The reaction was stopped by washing in water, and slides were counterstained also in the Benchmark XT machine with hematoxylin I or Bluing Reagent. CD20 has been used as pan-B cell marker and CD21 for follicular dendritic cells (FDCs), whereas CD21 may also stain mature B cells in frozen (and not paraffin-embedded) sections.

For Ig staining in human lungs, after disembedding and rehydration of the specimens, endogenous peroxidases were inhibited by incubation in 0.3% (vol/vol) H_2O_2 in water for 30 min, and the slides were treated with 1% (wt/vol) BSA in Tris-buffered saline for 30 min. The following Abs were used respectively for IgM, IgG and IgA staining: biotin-conjugated Abs goat anti-human IgM (B2641, Sigma, USA), rabbit anti-human IgG (Southern Biotech, USA) and unlabeled mouse anti-human IgA mAb (Thermo Scientific, USA) followed by streptavidin-HRP or anti-mouse HRP conjugated Ab. The reaction was developed by incubation with 0.6 mg/ml diaminobenzidine (SigmaFast DAB, Sigma, USA) in 0.3% H_2O_2 for 10 min. In murine lungs, rabbit anti-mouse IgG (Sigma B8520, USA) and biotinylated rat anti-mouse IgA (Sigma LO-MA-10, USA) Abs were used for detection. Revelation was performed as described above for human Igs.

Copyright © 2018 by the American Thoracic Society

AJRCCM Articles in Press. Published on 19-October-2018 as 10.1164/rccm.201802-0352OC

Staining quantification was carried out after digitalization with a x40 objective using the slide scanner SCN400 (Leica microsystems, Germany) and TissueIA software (Leica microsystems, Ireland). Quantification included application of algorithms for each immunostaining (Leica microsystems, Germany). Color deconvolution was applied to each pixel using hematoxylin and DAB or Fast Red matrix of the software. On the color matrix, a threshold was adjusted for DAB or Fast Red detection according to color intensity. These parameters were kept constant throughout the quantification for each immunostaining. For the quantification (percentage) of extrafollicular CD20 positive cells in whole sections, nuclear parameters (size, heterogeneity, strength of nuclear counterstaining, nuclei density) and cellular parameters (size and cell radius) were adjusted on the hematoxylin matrix to determine the adequate segmentation. Then, the number of DAB positive cells (CD20+ cells) was evaluated as a percentage of total cells. For quantification of CD20 (or CD21)+ LF, the number of positive aggregates was counted manually for each section, and results were adjusted to the tissue area analyzed per section. For the quantification of intra-LF Ig+ (IgM+, IgG+ or IgA+) B cells all LF were delineated manually and Ig+ B cells were counted within those LF. Hematoxylin segmentation and DAB deconvolution were applied as above. Two parameters were determined, namely percentage of Ig-positive cells (evaluating the proportion of surface IgX+ B cells among all B cells) and the staining concentration (representing the average intensity of positive pixels corrected to the LF surface, reflecting the intensity of IgX expression).

Immunofluorescence (IF). Paraffin embedded lung sections were processed into 5µm-thick sections and mounted on slides for staining. After classical deparaffinization and drying (toluene and methanol), antigen recovery was obtained by high pressure treatment (15 PSI during 15 min, in citrate buffer (pH 6.0)). Tissue sections were blocked with Bloxall® (Vector Laboratories, SP-6000) for 15 min and blocking serum for 30 min, then endogenous peroxidases were blocked by incubation with 0.3% H_2O_2 for 30 min. Afterwards, sections were

Copyright © 2018 by the American Thoracic Society

AJRCCM Articles in Press. Published on 19-October-2018 as 10.1164/rccm.201802-0352OC

successively stained and revealed for IL-21 (Merck-Millipore, 06-1074), BCL-6 (Acris, AM33123PUM), CXCR5 (Abcam, AB46218), CD3 (Cell Signaling, 85061S), and RORγt (Sigma, MABF81) by incubation with primary antibodies for 1.5 hour, poly-HRP conjugated secondary antibodies (Sigma, USA) for 1h, and tyramide-signal amplification reagents for 10 min. All staining preparations included a primary negative control IgG. Sections were scanned with the Pannoramic 250 Flash digital microscope (P250 Flash digital microscopes; 3DHISTECH, Budapest, Hungary).

RNA extraction and RT-qPCR. Total RNA was isolated from lung tissues using the Rneasy® Plus Mini kit (Qiagen, Hilden, Germany). Total RNA (500 ng per sample) was reverse-transcribed with RevertAidTM Reverse transcriptase kit (Fermentas, St. Leon-Rot, Germany) with 0.3 µg of random hexamer (Invitrogen, Gent, Belgium) and 1mM of each dNTP (Invitrogen, Gent, Belgium) following the manufacturer's protocol in a thermocycler (Applied Biosystems, Carlsbad, CA, USA). The expression levels in lung tissues of human IL-6 and IL-21 were assessed and reported to those of RPS18, RNA18S and GAPDH housekeeping genes (by using the geometric mean of the three housekeeping genes, HKG); as well as mouse IgA and IgG1 that were reported to those of RNA18S housekeeping gene. The quantification was made by real time quantitative PCR using the iCycler IQ5 PCR (Bio-Rad, Hercules, CA, USA). The reaction mix contained 5µl of 10-fold diluted cDNA, 400nM of each and 2x iQTM SYBR®Green Supermix (Bio-Rad, USA) in a final volume of 20µl. The cycling conditions were 95°C for 3 min followed by 40 cycles of 95°C for 15s and 60°C for 30s. To control the specificity of the amplification products, a melting curve analysis was performed. Samples were run in duplicates and the copy number was calculated from the standard curve. Data analysis was performed using Bio-Rad iQ5 Software (Bio-Rad, USA).

Copyright © 2018 by the American Thoracic Society

AJRCCM Articles in Press. Published on 19-October-2018 as 10.1164/rccm.201802-0352OC

Supplemental figures legends:

Figure E1: CD21 positive follicular Dendritic cells (fDCs) in proximal and distal lung tissue (A) Representative peri-bronchial lymphoid structure with red staining and blue hematoxylin counterstaining, and evaluation of **(B)** the number of CD21 positive lymphoid structures per tissue area in large airways in a subset of control and COPD patients with GOLD I-II and III-IV stages **(C)** Representative parenchymal lymphoid structure, and evaluation of **(D)** the number of CD21 positive lymphoid structures per tissue area in small airways. Among controls, non-smokers are represented by white circles, control ex-smokers and current smokers by black circles. Among COPD patients, white triangles represent GOLD I-II COPD and black triangles represent GOLD III-IV COPD. Lines represent median and interquartile range. Scale bar, 100μm.

Figure E2: Intra-follicular immunoglobulin expression in proximal lung tissue. (A), **(C)** and **(E)** Evaluation of the number of intra-follicular IgA, IgG or IgM positive cells (% of intra-follicular total cells) respectively and **(B)**, **(D)** and **(F)** the staining concentration of intra-follicular IgA, IgG or IgM staining (reported to the lymphoid structure surface area) in control and COPD patients with GOLD I-II and III-IV stages. Among controls, non-smokers are represented by white circles, control ex-smokers and current smokers by white and black triangles, respectively. Among COPD patients, white squares represent ex-smokers with GOLD I-II COPD and black squares active smokers with GOLD I-II COPD patients; white inverted triangles represent ex-smokers with GOLD III-IV COPD and black inverted triangles smokers with GOLD III-IV COPD. **(G)** Comparison between percentages of intra-follicular IgA, IgG and IgM positive cells in all pooled (control and COPD) groups. Mann-Whitney U test; * $p<0.05$, ** $p<0.01$, *** $p<0.001$.

Figure E3: Intra-follicular Immunoglobulin expression in distal lung tissue. (A), (C) and (E) Evaluation of the number of intra-follicular IgA, IgG or IgM positive cells (% of intra-

Copyright © 2018 by the American Thoracic Society

AJRCCM Articles in Press. Published on 19-October-2018 as 10.1164/rccm.201802-0352OC

follicular total cells) respectively and **(B), (D) and (F)** the staining concentration of intra-follicular IgA, IgG or IgM staining (reported to the lymphoid structure surface area) in control and COPD patients with GOLD I-II and III-IV stages. Among controls, non-smokers are represented by white circles, control ex-smokers and current smokers by white and black triangles, respectively. Among COPD patients, white squares represent ex-smokers with GOLD I-II COPD and black squares active smokers with GOLD I-II COPD patients; white inverted triangles represent ex-smokers with GOLD III-IV COPD and black inverted triangles smokers with GOLD III-IV COPD. **(G)** Comparison between percentages of intra-follicular IgA, IgG and IgM positive cells in all pooled (control and COPD) groups. **(H)** Correlation of intra-LF IgA + cells in distal lung with FEV1/FVC ration values in all groups. Mann-Whitney U test for comparisons and Spearman test for correlation; * $p<0.05$, ** $p<0.01$, *** $p<0.001$.

Figure E4: IgG expression in lung tissue and broncho-alveolar lavage from Pseudomonas infected mice. (A), **(B)** and **(C)** Representative IgG staining (brown) and hematoxylin counterstaining (blue) in lung tissue from non-immune control **IgG** staining, mice instilled with sterile beads or PAO1-infected mice, respectively; and evaluation of **(D)** and **(E)** total IgG expression and **(F)** intra-follicular IgG-positive cells at days 14 and 28 post-infection; **(G)** and **(H)** total and PAO-specific IgG in broncho-alveolar lavage from mice instilled with sterile beads or PAO-infected mice at day 14 post-infection; **(I)** IgG1 mRNA expression corrected to the housekeeping gene in lung tissue from mice instilled with sterile beads or PAO-infected mice at day 14 post-infection. White circle (mice instilled with sterile beads, n=5 to 9) and black circles (mice infected with PAO beads, n=5 to 10). Scale bar, 100µm. Lines represent median and interquartile range. Mann-Whitney U test; * $p<0.05$, ** $p<0.01$.

Figure E5: IgA and IgG expression in broncho-alveolar lavage (BAL) and lung tissue from smoking mice. Evaluation of **(A)** and **(B)** total IgA and IgG expression; **(C)** and **(D)** intra-follicular IgA and IgG expression in lung tissue of smoking versus non-smoking mice and **(E)**

Copyright © 2018 by the American Thoracic Society

AJRCCM Articles in Press. Published on 19-October-2018 as 10.1164/rccm.201802-0352OC

and **(F)** total IgA and IgG in broncho-alveolar lavage from smoking versus non-smoking mice. White circle (mice exposed to ambient air, n=8 to 11) and black circles (mice exposed to cigarette smoke, twice a day for 12 weeks, n=9 to 11). Lines represent median and interquartile range. Mann-Whitney U test; * $p<0.05$.

Copyright © 2018 by the American Thoracic Society

AJRCCM Articles in Press. Published on 19-October-2018 as 10.1164/rccm.201802-0352OC

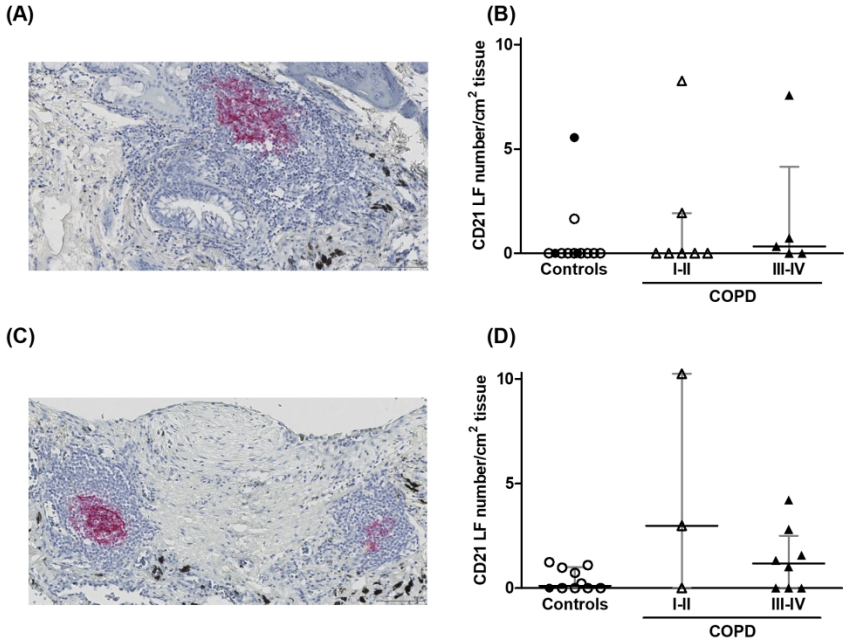

Figure E1

Figure E1: CD21 positive follicular Dendritic cells (fDCs) in proximal and distal lung tissue (A) Representative peri-bronchial lymphoid structure with red staining and blue hematoxylin counterstaining, and evaluation of (B) the number of CD21 positive lymphoid structures per tissue area in large airways in a subset of control and COPD patients with GOLD I-II and III-IV stages (C) Representative parenchymal lymphoid structure, and evaluation of (D) the number of CD21 positive lymphoid structures per tissue area in small airways. Among controls, non-smokers are represented by white circles, control ex-smokers and current smokers by black circles. Among COPD patients, white triangles represent GOLD I-II COPD and black triangles represent GOLD III-IV COPD. Lines represent median and interquartile range. Scale bar, 100μm.

190x254mm (300 x 300 DPI)

Copyright © 2018 by the American Thoracic Society

AJRCCM Articles in Press. Published on 19-October-2018 as 10.1164/rccm.201802-0352OC

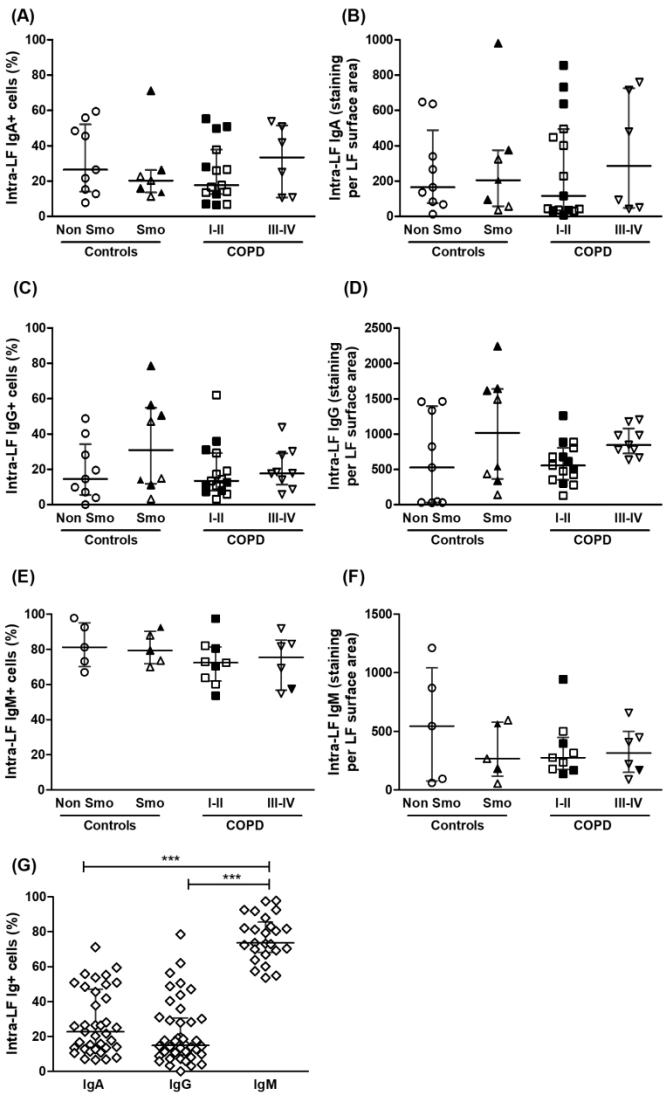

Figure E2

Figure E2: Intra-follicular immunoglobulin expression in proximal lung tissue. (A), (C) and (E) Evaluation of the number of intra-follicular IgA, IgG or IgM positive cells (% of intra-follicular total cells) respectively and (B), (D) and (F) the staining concentration of intra-follicular IgA, IgG or IgM staining (reported to the lymphoid structure surface area) in control and COPD patients with GOLD I-II and III-IV stages. Among controls, non-smokers are represented by white circles, control ex-smokers and current smokers by white and black triangles, respectively. Among COPD patients, white squares represent ex-smokers with GOLD I-II COPD and black squares active smokers with GOLD I-II COPD patients; white inverted triangles represent ex-smokers with GOLD III-IV COPD and black inverted triangles smokers with GOLD III-IV COPD. (G) Comparison between percentages of intra-follicular IgA, IgG and IgM positive cells in all pooled (control and COPD) groups. Mann-Whitney U test; * $p<0.05$, ** $p<0.01$, *** $p<0.001$.

190x254mm (300 x 300 DPI)

Copyright © 2018 by the American Thoracic Society

AJRCCM Articles in Press. Published on 19-October-2018 as 10.1164/rccm.201802-0352OC

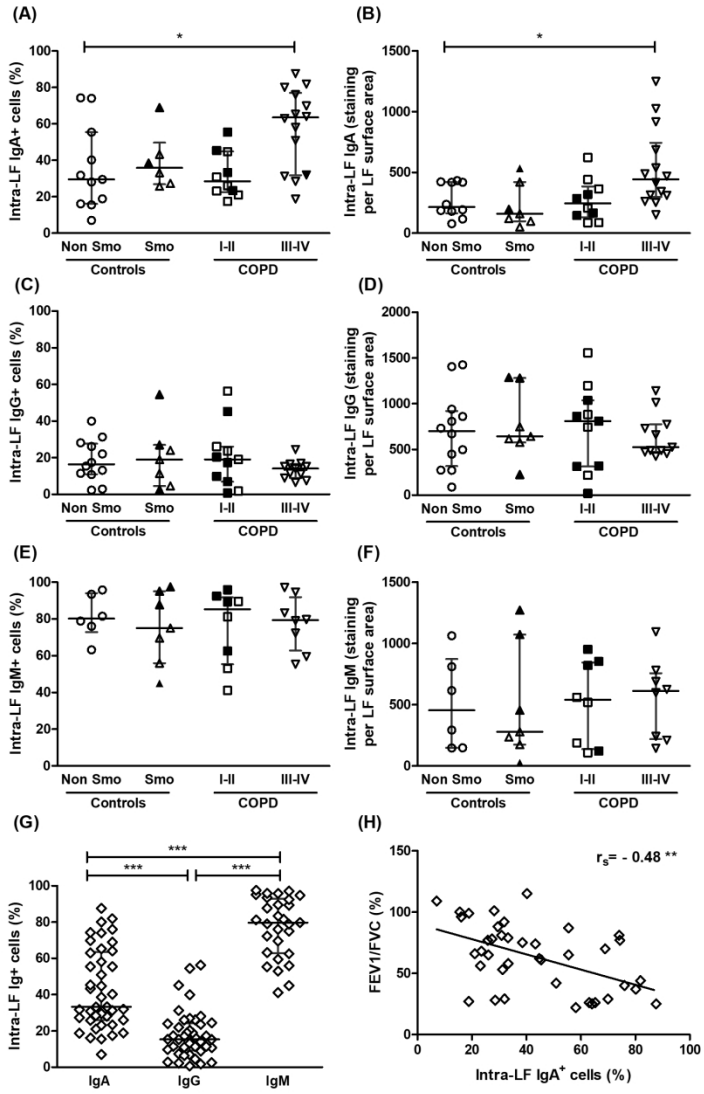

Figure E3

Figure E3: Intra-follicular Immunoglobulin expression in distal lung tissue. (A), (C) and (E) Evaluation of the number of intra-follicular IgA, IgG or IgM positive cells (% of intra-follicular total cells) respectively and (B), (D) and (F) the staining concentration of intra-follicular IgA, IgG or IgM staining (reported to the lymphoid structure surface area) in control and COPD patients with GOLD I-II and III-IV stages. Among controls, non-smokers are represented by white circles, control ex-smokers and current smokers by white and black triangles, respectively. Among COPD patients, white squares represent ex-smokers with GOLD I-II COPD and black squares active smokers with GOLD I-II COPD patients; white inverted triangles represent ex-smokers with GOLD III-IV COPD and black inverted triangles smokers with GOLD III-IV COPD. (G) Comparison between percentages of intra-follicular IgA, IgG and IgM positive cells in all pooled (control and COPD) groups. (H) Correlation of intra-LF IgA + cells in distal lung with FEV1/FVC ration values in all groups. Mann-Whitney U test for comparisons and Spearman test for correlation; * $p<0.05$, ** $p<0.01$, *** $p<0.001$.

190x254mm (300 x 300 DPI)

Copyright © 2018 by the American Thoracic Society

AJRCCM Articles in Press. Published on 19-October-2018 as 10.1164/rccm.201802-0352OC

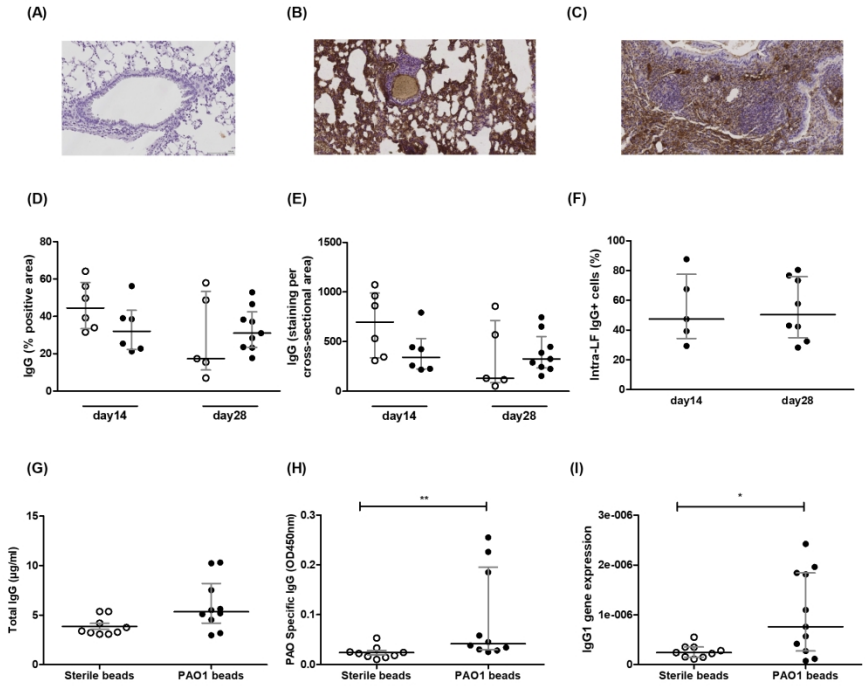

Figure E4

Figure E4: IgG expression in lung tissue and broncho-alveolar lavage from Pseudomonas infected mice. (A), (B) and (C) Representative IgG staining (brown) and hematoxylin counterstaining (blue) in lung tissue from non-immune control IgG staining, mice instilled with sterile beads or PAO1-infected mice, respectively; and evaluation of (D) and (E) total IgG expression and (F) intra-follicular IgG-positive cells at days 14 and 28 post-infection; (G) and (H) total and PAO-specific IgG in broncho-alveolar lavage from mice instilled with sterile beads or PAO-infected mice at day 14 post-infection; (I) IgG1 mRNA expression corrected to the housekeeping gene in lung tissue from mice instilled with sterile beads or PAO-infected mice at day 14 post-infection. White circle (mice instilled with sterile beads, n=5 to 9) and black circles (mice infected with PAO beads, n=5 to 10). Scale bar, 100µm. Lines represent median and interquartile range. Mann-Whitney U test; * $p<0.05$, ** $p<0.01$.

190x254mm (300 x 300 DPI)

Copyright © 2018 by the American Thoracic Society

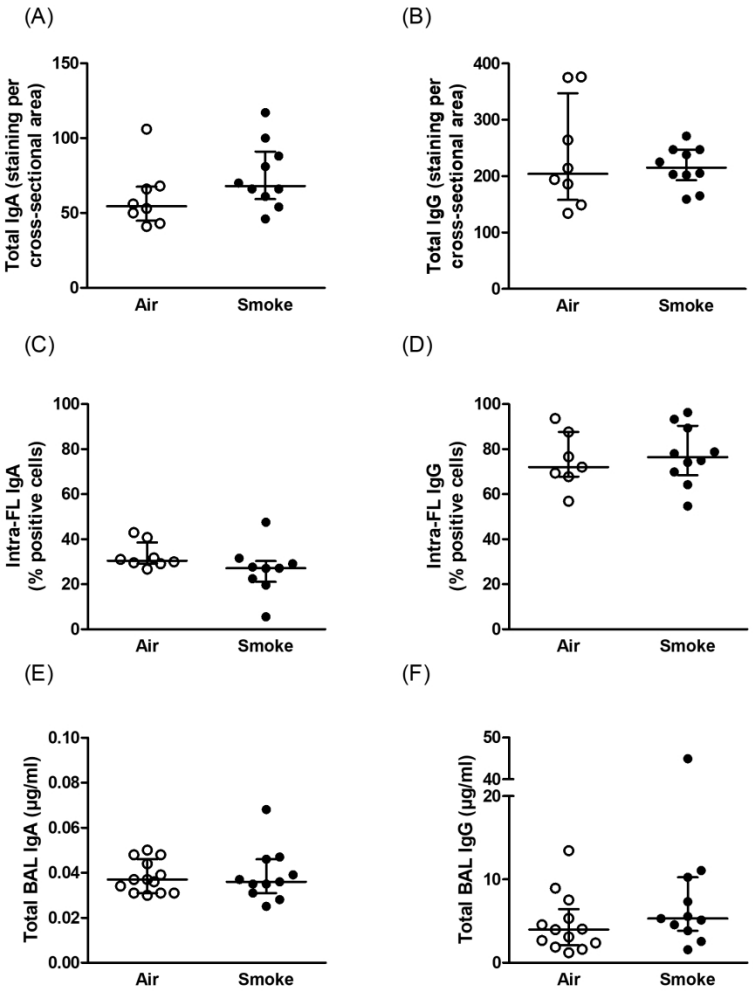

Figure E5

Figure E5: IgA and IgG expression in broncho-alveolar lavage (BAL) and lung tissue from smoking mice. Evaluation of (A) and (B) total IgA and IgG expression; (C) and (D) intra-follicular IgA and IgG expression in lung tissue of smoking versus non-smoking mice and (E) and (F) total IgA and IgG in broncho-alveolar lavage from smoking versus non-smoking mice. White circle (mice exposed to ambient air, n=8 to 11) and black circles (mice exposed to cigarette smoke, twice a day for 12 weeks, n=9 to 11). Lines represent median and interquartile range. Mann-Whitney U test; * $p<0.05$.

190x254mm (300 x 300 DPI)

Copyright © 2018 by the American Thoracic Society